Anisotropically Functionalized Carbon Nanotube Array Based Hygroscopic Scaffolds

Sehmus Ozden,[†] Liehui Ge,[†] Tharangattu N. Narayanan,[‡] Amelia H. C. Hart,[†] Hyunseung Yang,[§] Srividya Sridhar,[‖] Robert Vajtai,[†] and Pulickel M. Ajayan*,[†]

[†]Department of Material Science and NanoEngineering, Rice University, Houston, Texas 77005, United States
[‡]CSIR-Central Electrochemical Research Institute, Karaikudi 630006, India
[§]Department of Chemical and Biomolecular Engineering, Korea Institute of Science and Technology, Daejeon 305-701, Korea
[‖]Department of Physics, Delhi Technological University, Bawana Road, Delhi 110042, India

ⓢ *Supporting Information*

ABSTRACT: Creating ordered microstructures with hydrophobic and hydrophilic moieties that enable the collection and storage of small water droplets from the atmosphere, mimicking structures that exist in insects, such as the Stenocara beetle, which live in environments with limited amounts of water. Inspired by this approach, vertically aligned multiwalled carbon nanotube forests (NTFs) are asymmetrically end-functionalized to create hygroscopic scaffolds for water harvesting and storage from atmospheric air. One side of the NTF is made hydrophilic, which captures water from the atmosphere, and the other side is made superhydrophobic, which prevents water from escaping and the forest from collapsing. To understand how water penetrates into the NTF, the fundamentals of water/NTF surface interaction are discussed.

KEYWORDS: *carbon nanotubes, water harvesting, asymmetric functionalization, hydrophobic, hydrophilic*
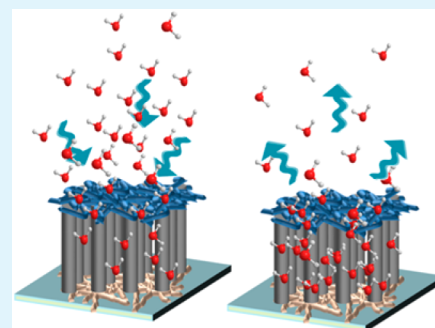
■ INTRODUCTION

Fresh water is an ever-decreasing resource that can be found in small amounts in almost every environment. In nature, there are many organisms, such as the Stenocara beetle, which lives in the Namib Desert and survives by drinking fogwater that collects on its wing case.[1] The unique design of the Stenocara beetle's back involves randomly spaced bumps with hydrophilic peaks surrounded by hydrophobic areas that guide water into its mouth. The Stenocara beetle stands on a sand dune, facing into the morning wind at a 45° angle. With its head facing downward and its bottom upward, the minute water droplets from the fog collect on the superhydrophilic peak of each bump. When the water droplets grow big enough, they detach from the bump peaks, fall onto the superhydrophobic areas between the bump peaks, and are guided downward to the beetle's mouth.[1] Additionally, Stipagrostis Sabulicola[2] and Cotula Fallax[3] are some other organisms that are able to effectively capture water droplets from the fog of the morning desert by using hydrophilic/hydrophobic combinations. In the recent past, a few efforts have been done using these and other hydrophilic/hydrophobic biomimetic mechanisms to capture and harvest atmospheric water[4−13] that do not require significant amounts of energy. Up to now, several approaches have been reported to create hydrophilic/hydrophobic surfaces for water harvesting. In these reports, polymers have been extensively used. For example, Zhai et al. mimicked the Stenocara beetle by creating hydrophilic patterns on superhydrophobic surfaces using hydrophilic and hydrophobic polymers.[14]

Another material that can be used for water harvesting is carbon nanotubes (CNTs). Known for their small size and mechanical and physical strength, CNTs can be easily made hydrophilic or superhydrophobic by chemical functionalization.[15,16] Several kinds of CNT functionalizations, such as covalent[17] and noncovalent functionalization,[18] have been reported extensively. Another type of CNT functionalization is asymmetric end functinalization, which attaches two different functionals at their opposite ends.[19] Even though some work has been reported, it is still a big challenge to functionalize two end tips with different functional groups.[19,20] For example, Lee et al. have used UV irradiation to attach different functional groups to opposite ends of individual CNTs.[19]

In order to harvest water, the material must consist of both hydrophilic and hydrophobic surfaces. For example, Kinoshita and co-workers used micropatterning on CNT films to create superhydrophobic—hydrophilic heterogeneous surfaces using plasma-type hydrothermal atom beams.[15] Here we report a new approach for anisotrophically functionalized carbon nanotube forest (NTF) as superhydrophilic/superhydrophobic. Because of the combination of hydrophilic and hydrophobic surfaces, we were able to utilize the material for water collection from dry air and high-humidity air. By this approach, the water microparticles in air can be captured and stored in comparatively large amounts.
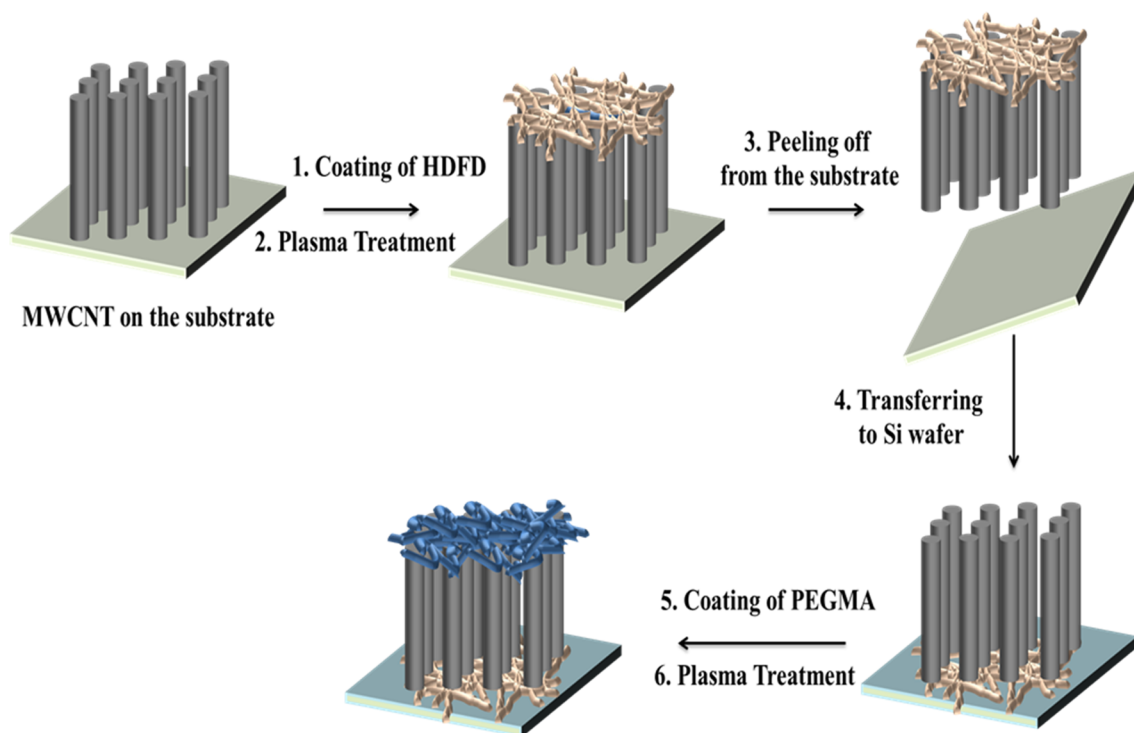
Figure 1. Schematic representation of asymmetric end functionalization of NTF. The top surface of the forest was coated with HDFD monomer and plasma-treated for 2 min. NTF was flipped over to another substrate, coated with PEGMA, and plasma-treated for 2 min.

■ EXPERIMENTAL SECTION

The NTFs were synthesized via water-assisted chemical vapor deposition (CVD) on a silica substrate, described elsewhere;[21] they were grown for 3 h, resulting in a height of ∼1 cm. Prior to CNT growth, 10-nm-thick aluminum buffer and iron catalyst layers were deposited on the silica wafer using electron-beam (E-beam) evaporation. The CNT synthesis takes place at 775 °C under Ar/H_2 with ethylene as the carbon source and a water bubbler to aid in the removal of amorphous carbon.

To create the hydrophobically functionalized side of the NTF, $1H,1H,2H$-heptadecafluoro-1-decene (HDFD; 99%, Sigma-Aldrich) was coated onto the top surface of the as-grown NTF and plasma-treated (700 V direct current) for 2 min. After this, the NTF was then removed from the silica substrate, flipped over, and transferred to a new silica substrate for further functionalization on the bottom surface. For hydrophilic functionalization on the opposite side of the NTF, 0.5 mL of poly(ethylene glycol) methacrylate (PEGMA) monomer (average M_n = 360; Sigma-Aldrich) was coated onto the surface, and the NTF was plasma-treated (700 V direct current) for 2 min (Figure 1). For comparison, one hydrophobically/hydrophilically functionalized NTF (PEGMA/HDFD-NTF), one NTF only hydrophilically PEGMA functionalized (PEGMA/PEGMA-NTF) on both top and bottom, one NTF only top side functionalized with PEGMA (PEGMA-NTF), and one nonfunctionalized NTF were all tested for water harvesting. Characterization was performed using scanning electron microscopy (SEM; FEI Quanta 400 ESEM FEG), Raman spectroscopy, X-ray photoelectron spectroscopy (XPS), thermogravimetric analysis (TGA), Fourier transform infrared spectroscopy (FT-IR), and contact-angle measurements.

■ RESULTS AND DISCUSSION

To confirm that the NTF is actually hydrophilic/hydrophobic asymmetrically end-functionalized, the contact angle of each side is measured and discussed. The three different stages of functionalization—as-grown NTF, HDFD-NTF, and PEGMA-NTF—can be seen in the SEM images shown in parts a–c of Figure 2, respectively. As seen in the inset of the three figures, the contact angle increases with HDFD treatment

[118° (as-grown NTF) to 162° (superhydrophobic)] and becomes completely hydrophilic after PEGMA treatment (0°). As seen in Figure 2, the surface roughness of the end-functionalized NTF also affects the hydrophobicity and hydrophilicity of the surfaces;[22] a hydrophobic/hydrophilic surface becomes superhydrophobic/superhydrophilic with larger surface roughness.[22] It is also important to note that infiltration of the organic monomers and plasma treatment for polymerization only functionalize the ends of the CNTs up to a few micrometers in depth (Figure 3a,b), which creates a CNT pot/container.

An additional way to evidence the success of hydrophilic/hydrophobic functionalization of the NTF is Raman and IR spectroscopy, XPS, and TGA. As seen in Figure 4a, upon comparison of the Raman spectra of the as-grown NTF to that of PEGMA-CNT and HDFD-NTF, the G band, the in-plane vibration of the C−C bond, the D band, which shows the structural defects,[23] and the G′ band, the second-order overtone of the D band, all upshifted because of intercalation of the polymer with the CNT bundles.[24] In Figure S1 in the Supporting Information (SI), the IR spectrum of HDFD-NTF shows a characteristic perfluoroalkyl chain, $-CF_2-$ stretching, between 1087 and 1245 cm^{-1} and a CF_3 stretching band around 1350 cm^{-1}.[25] On the PEGMA-NTF side, the IR spectrum shows an ether stretching band around 1735 cm^{-1} and alkyl chain CH_2 and CH_3 stretching bands at 2892 and 2977 cm^{-1}, respectively. XPS analysis, performed for quantitative chemical analysis, of the as-grown NTF (Figure 4b) shows sp^2 C atoms at approximately 284.6 eV, and peaks at 284.9 and 285.4 eV represent C=O and C−O bonds, respectively. A weak oxygen peak at around 532 eV is shown in Figure S8 in the SI. In the XPS spectrum of HDFD-NTF (Figure 4c), the C 1s spectrum corresponds to graphitic carbon and the shoulder peak at 286.5 eV shows C−CF bonding. The peak at 291.8 eV represents CF_2 bonding, and CF_3 bonding is seen at around 294 eV. There are two C 1s peaks in XPS
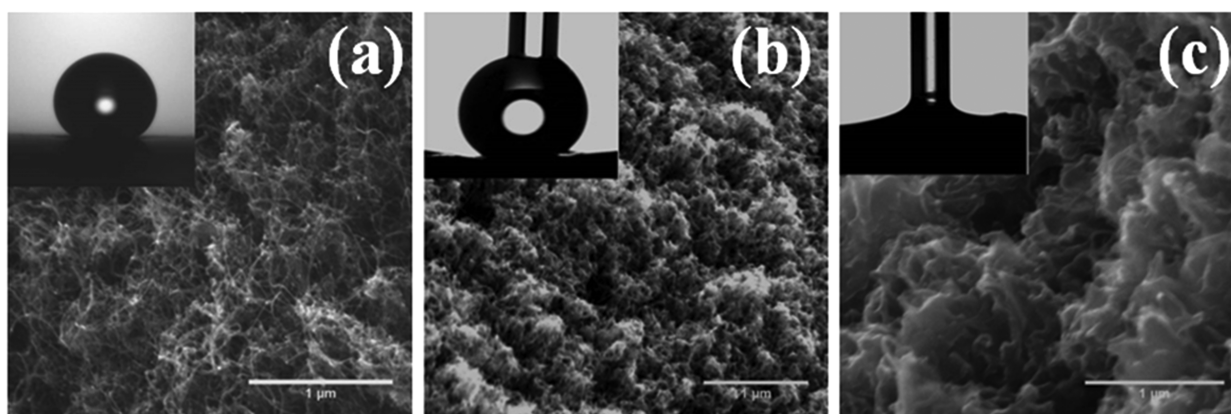
Figure 2. SEM images of (a) as-grown NTF (contact angle of the CNTs is 118°), (b) HDFD-NTF (contact angle is increased to 162°, which is a superhydrophobic surface), and (c) PEGMA-NTF (contact angle decreased to 0°, which is superhydrophilic). Polymerization on the surface clearly can be seen after plasma treatment.
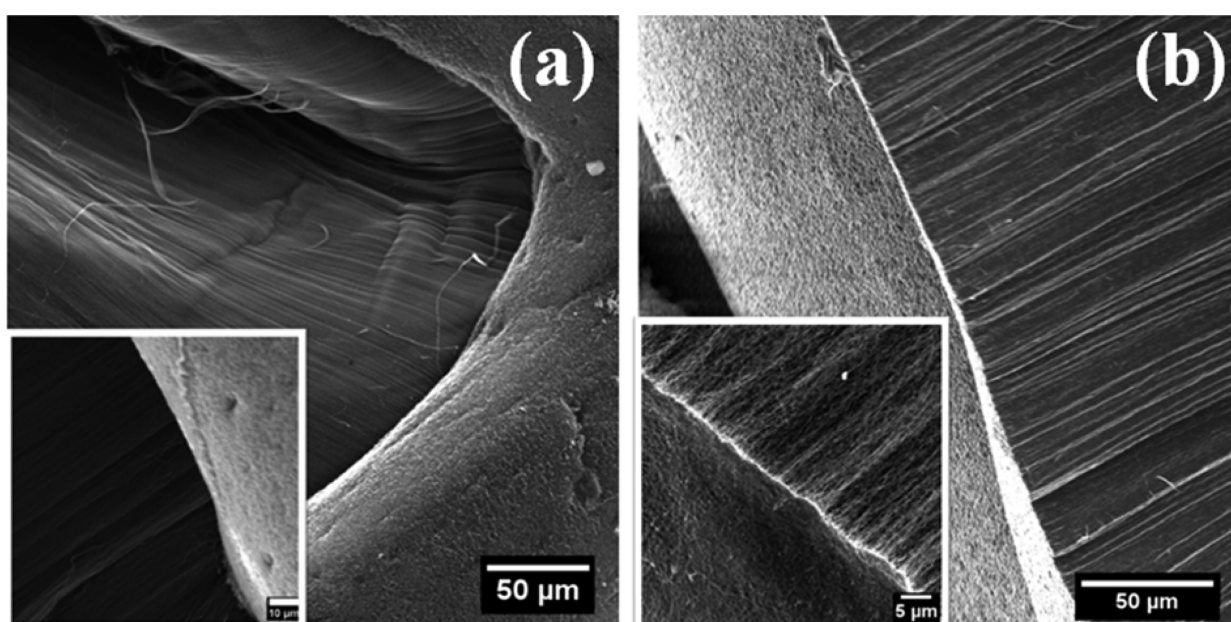

Figure 3. SEM images of (a) HDFD-NTF (superhydrophobic side) and (b) PEGMA-NTF (superhydrophilic side). It can clearly be seen that polymers penetrate a few micrometers into the CNT because monomers penetrate into the forest during coating. If the amount of monomers increase, the penetration will be deeper.

analysis of PEGMA-NTF at 285 and 286.5 eV, corresponding to CO and CH_2 (Figure 4d) and a peak at 289 eV representing $O-C=O$ bonding.[26,27] PEGMA-NTF has a larger amount of O atoms than the as-grown NTF because of the contribution of carbonyl ($C=O$) and ether ($C-O$) functional groups in PEGMA. TGA, conducted in an Ar atmosphere (10 °C/min; Figure S2 in the SI), shows that the PEGMA-CNT and HDFD-CNT sides of the forest start to decompose around 230 and 600 °C, respectively.

To demonstrate its water-harvesting capabilities, the PEGMA/HDFD-NTF samples were exposed to dry and humid air at room temperature and weighed before and throughout the experiment. During testing, PEGMA/HDFD-NTF was oriented so that the hydrophilic PEGMA-treated surface remained facing upward, to capture the water, and the superhydrophobic HDFD-treated surface remained facing downward, to hold the water. Four types of samples were tested: PEGMA/HDFD-NTF, PEGMA/PEGMA-NTF, PEGMA-NTF, and as-grown NTF. The first test was performed in dry air [21% relative humidity (RH)] for

11 h and weighed every 1 h. The second test was performed under very humid air (89% RH), generated by a water bubbler (Figure S5 in the SI), for 13 h and weighed every 1 h.

To measure the water evaporation (WE) rate, 1 mL of water was dropped onto the hydrophilic side of PEGMA/HDFD-NTF and weight measurements were taken every 1 h at room temperature as well as under heating (40 °C). To compare this rate to the normal WE rate, a separate glass vessel (0.5 cm diameter) was tested simultaneously. These results show that the evaporation rate of water in the asymmetrically functionalized NTF is slower than that in a solid vessel because the asymmetrically functionalized NTF is able to isolate water from the external environment.

It was found, during the first water-harvesting and storage test, seen in Figure 5a, that PEGMA/HDFD-NTF with a 0.5 cm × 0.5 cm surface (~8 mg) harvests 27.4 wt % (~2.27 mg) of water from the air in 11 h. In the second test performed under high RH, also seen in Figure 5a, PEGMA/HDFD-NTF collected 80 wt % (~6.4 mg) of water in 13 h. PEGMA-NTF, tested under
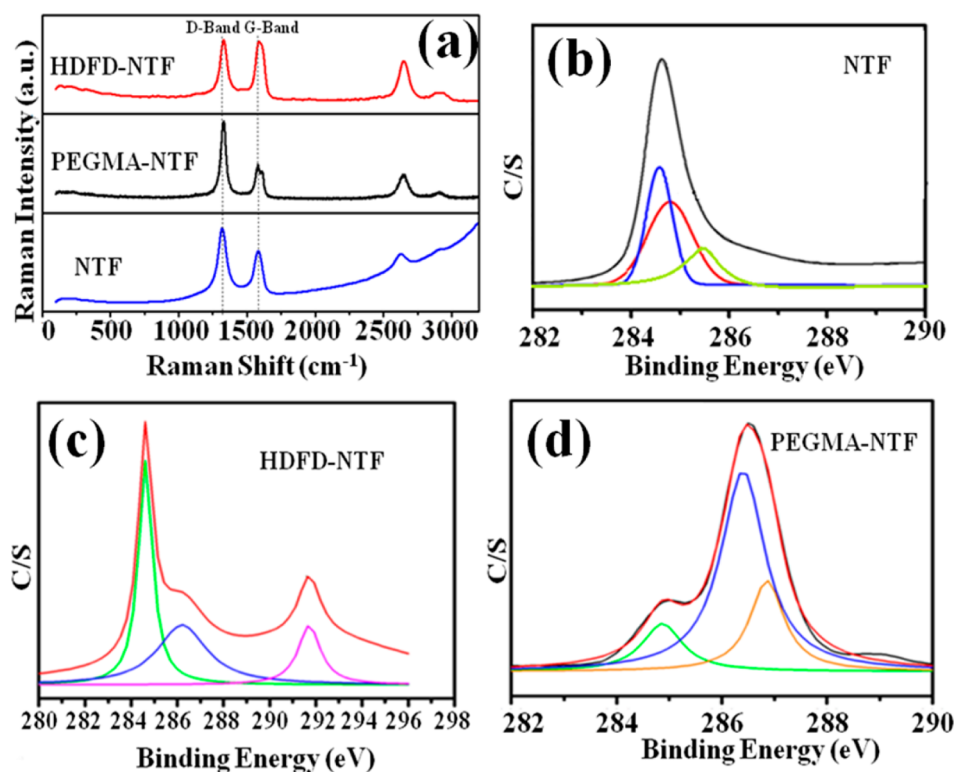
Figure 4. (a) Raman spectra of as-grown and asymmetrically functionalized NTF. XPS spectra of (b) as-grown NTF, (c) HDFD-NTF (superhydrophobic), and (d) PEGMA-NTF (superhydrophilic).
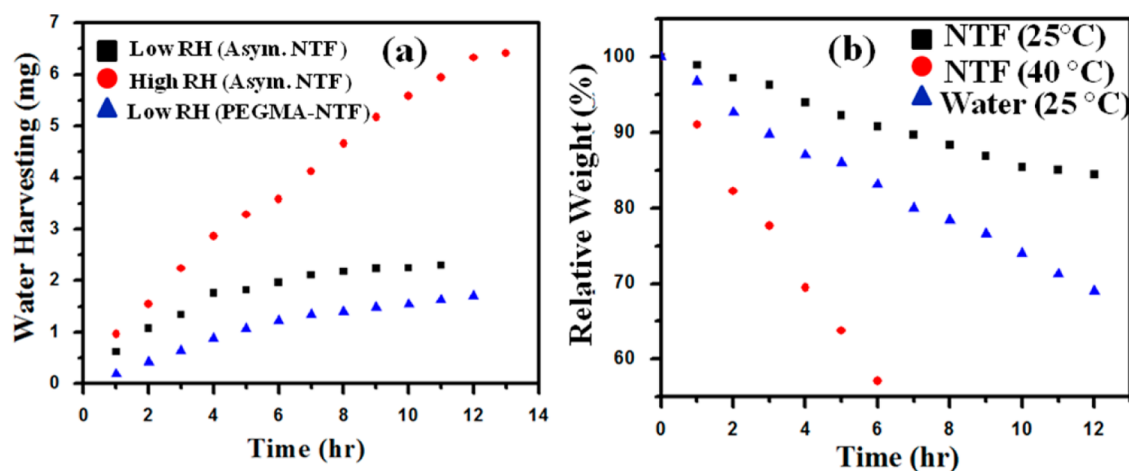

Figure 5. (a) Harvesting water from a low RH rate and a high RH rate. (b) WE rate of water from asymmetrically functionalized NTF and from a vessel.

the same conditions, collected ~6.4 mg of water in 13 h, but the nonfunctionalized side of NTF collapsed, leading to destruction of the entire forest (Figure S3 in the SI) . The HDFD and PEGMA polymers prevent destruction of NTF due to covalent bonding between the CNTs and polymers. PEGMA/PEGMA-NTF was not able to store water; water was dropped onto the hydrophilic top and escaped from the hydrophilic bottom side. After undergoing the same testing, as-grown NTF shows no weight difference because of the hydrophobic nature of the entire forest.

In order to understand how water penetrates and stores in the NTF, it is important to understand the interactions between the water molecules and hydrophilic PEGMA or hydrophobic HDFD surfaces, respectively. Water is a polar molecule, where the hydrogen bonding keeping the atoms together is constantly breaking and forming bonds with new molecules.

The hydrophilic PEGMA surface consists of polar oxygen-containing functional groups ($-$OH, $-$C$=$O, C$-$O$-$C), which absorb water due to hydrogen bonding, van der Waals forces, and dipole$-$dipole interactions between the superhydrophilic surface and water molecules. Water that is liquid, meaning it has a small contact angle on surfaces, will spontaneously condense from vapor into pores on the superhydrophilic forest side.[28] Because the adhesive forces between the water molecules and the hydrophilic surface of NTF are stronger than the cohesive forces, the water molecules are able to spread over the PEGMA-NTF surface. A water molecule attracts other molecules, which surround it, and, in turn, is attracted by them. For water molecules that are inside a liquid, the result of all of these forces is neutral, and the molecules are equally attracted to each other. When these molecules are on the surface, they are attracted by the water

molecules that are below and by lateral ones. As a result of these attractions, water molecules are directed inside the liquid[28] (Figure S6 in the SI).

Capillary force, gravitational force, and pressure balance models can be used to predict the penetration of water into PEGMA/HDFD-NTF. The pressure balance model, which can be effective for water penetration into PEGMA/HDFD-NTF, is based on the assumption that when water wets PEGMA-NTF, the air in NTF is not expelled but compressed.[29,30] At the liquid–air interface, a force balance exists between the force exerted by the compressed air and the sum of the capillary force and gravitational force.[30] The capillary force F_C can be expressed as

$$F_C = \gamma \pi d \cos \theta \tag{1}$$

where γ, d, and θ are the surface tension of the water, pore diameter, and Young's contact angle, respectively.[31] The gravitational force is relatively small compared to the capillary force, so the capillary force is balanced by the air resistance. The amount of absorbed vapor is dependent on the temperature and RH in the atmosphere. The lotus effect protects the superhydrophobic surface of NTF from wetting as well as the hydrophobic side walls of NTF, so the water is retained inside the forest. The asymmetrically functionalized ends of NTF remain aligned because CNTs are covalently bonded via polymer chains. As a result of all of the above, the asymmetrically functionalized NTF behaves as a container; NTF holds water because of the innate hydrophobicity of CNTs and the superhydrophobic nonwetting bottom surface of the functionalized NTF (Figure S7 in the SI).

During the WE measurements, seen in Figure 5b, it was found that the WE rate in the end-functionalized NTF was less than that in an open vessel. At room temperature, after 6 h, the end-functionalized NTF lost ∼8% of its weight compared to the 60% water weight lost by the vessel in 6 h. At 40 °C, the end-functionalized NTF lost 40% of its weight in 6 h. The reasons for this lower WE rate are the polymer from functionalization prevents water from evaporating (Figure S4 in the SI) and NTF holds the water molecules captive, preventing evaporation.

CONCLUSION

To conclude, NTF was asymmetrically functionalized as hydrophilic and superhydrophobic via plasma treatment after coating with HDFD and PEGMA monomers on either side. The hydrophobic surface became more hydrophobic and the hydrophilic surface became more hydrophilic because of increased surface roughness. The asymmetrically functionalized NTF efficiently harvests and stores water from air humidity because of its superhydrophobic bottom surface, superhydrophilic top surface, and innate hydrophobicity of the center. In the future, it is possible to apply this unique system to arid lands if NTF productions become cheaper and scalable because this system, unlike other water collection devices, does not require an external energy source for collecting water from humid ambient air.

ASSOCIATED CONTENT

S Supporting Information

FT-IR spectra of as-grown NTF, HDFD-NTF, and PEGMA-NTF, TGA of asymmetrically functionalized NTF, images of asymmetrically functionalized NTF after water harvesting, schematic figure of water storage of asymmetrically end-functionalized NTF, schematic representation of water harvesting in a high-humidity chamber, figure of interactions between water molecules and hydrophilic surfaces, schematic representation that explains the water storage mechanism in NTF, and a

survey scan of XPS characterization of NTF, HDFD-NTF, and PEGMA-NTF. This material is available free of charge via the Internet at http://pubs.acs.org.

AUTHOR INFORMATION

Corresponding Author
*E-mail: ajayan@rice.edu.

Notes
The authors declare no competing financial interest.

ACKNOWLEDGMENTS

REFERENCES

(1) Parker, A. R.; Lawrence, C. R. Water Capture by a Desert Beetle. *Nature* **2001**, *414*, 33−34.

(2) Ebner, M.; Miranda, T.; Roth-Nebelsick, A. Efficient Fog Harvesting by Stipagrostis Sabulicola (Namib Dune Bushman Grass). *J. Arid Environ.* **2011**, *75*, 524−531.

(3) Andrews, H. G.; Eccles, E. A.; Schofield, W. C. E.; Badyal, J. P. S. Three-Dimensional Hierarchical Structures for Fog Harvesting. *Langmuir* **2011**, *27*, 3798−802.

(4) Lee, A.; Moon, M. W.; Lim, H.; Kim, W. D.; Kim, H. Y. Water Harvest via Dewing. *Langmuir* **2012**, *28*, 10183−91.

(5) Thickett, S. C.; Neto, C.; Harris, A. T. Biomimetic Surface Coatings for Atmospheric Water Capture Prepared by Dewetting of Polymer Films. *Adv. Mater.* **2011**, *23*, 3718−3722.

(6) Bai, H.; Ju, J.; Zheng, Y. M.; Jiang, L. Functional Fibers with Unique Wettability Inspired by Spider Silks. *Adv. Mater.* **2012**, *24*, 2786−2791.

(7) Tian, X. L.; Chen, Y.; Zheng, Y. M.; Bai, H.; Jiang, L. Controlling Water Capture of Bioinspired Fibers with Hump Structures. *Adv. Mater.* **2011**, *23*, 5486−5491.

(8) Zheng, Y. M.; Bai, H.; Huang, Z. B.; Tian, X. L.; Nie, F. Q.; Zhao, Y.; Zhai, J.; Jiang, L. Directional Water Collection on Wetted Spider Silk. *Nature* **2010**, *463*, 640−643.

(9) Hou, Y. P.; Chen, Y.; Xue, Y.; Zheng, Y. M.; Jiang, L. Water Collection Behavior and Hanging Ability of Bioinspired Fiber. *Langmuir* **2012**, *28*, 4737−4743.

(10) Gao, X. F.; Jiang, L. Water-Repellent Legs of Water Striders. *Nature* **2004**, *432*, 36−36.

(11) Norgaard, T.; Dacke, M. Fog-Basking Behaviour and Water Collection Efficiency in Namib Desert Darkling Beetles. *Front Zool.* **2010**, *7*, 1−8.

(12) Feng, L.; Li, S. H.; Li, Y. S.; Li, H. J.; Zhang, L. J.; Zhai, J.; Song, Y. L.; Liu, B. Q.; Jiang, L.; Zhu, D. B. Super-Hydrophobic Surfaces: From Natural to Artificial. *Adv. Mater.* **2002**, *14*, 1857−1860.

(13) Rykaczewski, K.; Scott, J. H. J.; Rajauria, S.; Chinn, J.; Chinn, A. M.; Jones, W. Three Dimensional Aspects of Droplet Coalescence During Dropwise Condensation on Superhydrophobic Surfaces. *Soft Matter* **2011**, *7*, 8749−8752.

(14) Zhai, L.; Berg, M. C.; Cebeci, F. C.; Kim, Y.; Milwid, J. M.; Rubner, M. F.; Cohen, R. E. Patterned Superhydrophobic surfaces: Toward a Synthetic Mimic of the Namib Desert Beetle. *Nano Lett.* **2006**, *6*, 1213−1217.

(15) Kinoshita, H.; Ogasahara, A.; Fukuda, Y.; Ohmae, N. Super-hydrophobic/Superhydrophilic Micropatterning on a Carbon Nanotube Film Using a Laser Plasma-Type Hyperthermal Atom Beam Facility. *Carbon* **2010**, *48*, 4403−4408.

(16) Pastine, S. J.; Okawa, D.; Kessler, B.; Rolandi, M.; Llorente, M.; Zettl, A.; Frechet, J. M. J. A Facile and Patternable Method for the Surface Modification of Carbon Nanotube Forests Using Perfluoroarylazides. *J. Am. Chem. Soc.* **2008**, *130*, 4238−4239.

(17) Singh, P.; Campidelli, S.; Giordani, S.; Bonifazi, D.; Bianco, A.; Prato, M. Organic Functionalisation and Characterisation of Single-Walled Carbon Nanotubes. *Chem. Soc. Rev.* **2009**, *38*, 2214−2230.

(18) Simmons, T. J.; Bult, J.; Hashim, D. P.; Linhardt, R. J.; Ajayan, P. M. Noncovalent Functionalization as an Alternative to Oxidative Acid Treatment of Single Wall Carbon Nanotubes with Applications for Polymer Composites. *ACS Nano* **2009**, *3*, 865−870.

(19) Lee, K. M.; Li, L.; Dai, L. Asymmetric End-Functionalization of Multi-Walled Carbon Nanotubes. *J. Am. Chem. Soc.* **2005**, *127*, 4122−3.

(20) Peng, Q.; Qu, L. T.; Dai, L. M.; Park, K.; Vaia, R. A. Asymmetrically Charged Carbon Nanotubes by Controlled Functionalization. *ACS Nano* **2008**, *2*, 1833−1840.

(21) Ci, L.; Vajtai, R.; Ajayan, P. M. Vertically Aligned Large-Diameter Double-Walled Carbon Nanotube Arrays Having Ultralow Density. *J. Phys. Chem. C* **2007**, *111*, 9077−9080.

(22) Quere, D. Rough Ideas on Wetting. *Physica A* **2002**, *313*, 32−46.

(23) Osswald, S.; Havel, M.; Gogotsi, Y. Monitoring Oxidation of Multiwalled Carbon Nanotubes by Raman Spectroscopy. *J. Raman Spectrosc.* **2007**, *38*, 728−736.

(24) Zhao, Q.; Wagner, H. D. Raman spectroscopy of carbon-nanotube-based composites. *Philos. Trans. R. Soc., A* **2004**, *362*, 2407−2424.

(25) Badge, I.; Sethi, S.; Dhinojwala, A. Carbon Nanotube-Based Robust Steamphobic Surfaces. *Langmuir* **2011**, *27*, 14726−14731.

(26) Akhtar, M. S.; Chun, J. M.; Yang, O. B. Advanced Composite Gel Electrolytes Prepared with Titania Nanotube Fillers in Polyethylene Glycol for the Solid-State Dye-Sensitized Solar Cell. *Electrochem. Commun.* **2007**, *9*, 2833−2837.

(27) Okpalugo, T. I. T.; Papakonstantinou, P.; Murphy, H.; McLaughlin, J.; Brown, N. M. D. High Resolution XPS Characterization of Chemical Functionalised MWCNTs and SWCNTs. *Carbon* **2005**, *43*, 153−161.

(28) Israelachvili, J. N. *Intermolecular and Surface Forces*, 3rd ed.; Academic Press: London, 2011.

(29) Mateo, J. N.; Kulkarni, S. S.; Das, L.; Bandyopadhyay, S.; Tepper, G. C.; Wynne, K. J.; Bandyopadhyay, S. Wetting Behavior of Polymer Coated Nanoporous Anodic Alumina Films: Transition from Super-Hydrophilicity to Super-Hydrophobicity. *Nanotechnology* **2011**, *22*, 1−10.

(30) Buijnsters, J. G.; Zhong, R.; Tsyntsaru, N.; Celis, J. P. Surface Wettability of Macroporous Anodized Aluminum Oxide. *ACS Appl. Mater. Interfaces* **2013**, *5*, 3224−3233.

(31) Kwok, D. Y.; Neumann, A. W. Contact Angle Measurement and Contact Angle Interpretation. *Adv. Colloid Interface Sci.* **1999**, *81*, 167−249.